Structural magnetic glassiness in the spin ice $Dy_2Ti_2O_7$

Anjana M. Samarakoon,[1,2] André Sokolowski,[3] Bastian Klemke,[3] Ralf Feyerherm,[3] Michael Meissner,[3] R. A. Borzi,[4] Feng Ye,[5] Qiang Zhang,[5] Zhiling Dun,[6] Haidong Zhou,[6] T. Egami,[2,7,6] Jonathan N. Hallén,[8,9] Ludovic Jaubert,[10] Claudio Castelnovo,[8] Roderich Moessner,[9] S. A. Grigera,[4,*] and D. Alan Tennant[5,11,2,†]

[1]*Materials Science Division, Argonne National Laboratory, Argonne, Illinois 60439, USA*
[2]*Shull Wollan Center – A Joint Institute for Neutron Sciences, Oak Ridge National Laboratory, Oak Ridge, Tennessee 37831, USA*
[3]*Helmholtz-Zentrum Berlin für Materialien und Energie, D-14109 Berlin, Germany*
[4]*Instituto de Física de Líquidos y Sistemas Biológicos, UNLP-CONICET, La Plata 1900, Argentina*
[5]*Neutron Scattering Division, Oak Ridge National Laboratory, Oak Ridge, Tennessee 37831, USA*
[6]*Department of Materials Science and Engineering and Department of Physics and Astronomy, University of Tennessee, Knoxville, Tennessee 37996, USA*
[7]*Materials Science and Technology Division, Oak Ridge National Laboratory, Oak Ridge, Tennessee 37831,USA*
[8]*TCM Group, Cavendish Laboratory, University of Cambridge, Cambridge CB3 0HE, United Kingdom*
[9]*Max Planck Institute for the Physics of Complex Systems, 01187 Dresden, Germany*
[10]*CNRS, Université de Bordeaux, LOMA, UMR 5798, 33400 Talence, France*
[11]*Quantum Science Center, Oak Ridge National Laboratory, Oak Ridge, Tennessee 37821, USA*

(Received 6 April 2022; revised 1 July 2022; accepted 6 July 2022; published 29 August 2022)

The origin and nature of glassy dynamics presents one of the central enigmas of condensed-matter physics across a broad range of systems ranging from window glass to spin glasses. The spin-ice compound $Dy_2Ti_2O_7$, which is perhaps best known as hosting a three-dimensional Coulomb spin liquid with magnetically charged monopole excitations, also falls out of equilibrium at low temperature. How and why it does so remains an open question. Based on an analysis of low-temperature diffuse neutron-scattering experiments employing different cooling protocols alongside recent magnetic noise studies, combined with extensive numerical modeling, we argue that upon cooling, the spins freeze into what may be termed a "structural magnetic glass," without an *a priori* need for chemical or structural disorder. Specifically, our model indicates the presence of frustration on two levels, first producing a near-degenerate constrained manifold inside which phase ordering kinetics is in turn frustrated. A remarkable feature is that monopoles act as sole annealers of the spin network and their pathways and history encode the development of glass dynamics, allowing the glass formation to be visualized. Our results suggest that spin ice $Dy_2Ti_2O_7$ provides one prototype of magnetic glass formation specifically and a setting for the study of kinetically constrained systems more generally.

DOI: 10.1103/PhysRevResearch.4.033159

I. INTRODUCTION

Magnetism provides a remarkable playground for understanding complex phenomena. A wide variety of materials with spin networks that closely match theoretical models as well as the intuitive nature of spin degrees of freedom account for their wide-ranging importance. Spin glasses are a celebrated instance of this as examples of states where equilibrium breaks down. More recently, fractional quasiparticles and spin liquids have come into focus as scenarios where exotic phases emerge from highly frustrated landscapes. The observation of anomalous noise and development of memory effects in the highly frustrated spin-ice compound $Dy_2Ti_2O_7$ [1] point to a close connection between these. Given that an essential component of conventional spin glasses, namely, randomness, is believed to be absent, the prospect of a spin realization of a structural glass instead is a tantalizing prospect, especially given the simplifications a spin model could bring.

Spin liquids [2,3], unlike paramagnets, are not simply thermally disordered. Rather, they are characterized by a huge density of low-energy spin states. These can incorporate intricate correlations which emerge from local constraints imposed by competing interactions. At low temperature they can thus be fundamentally different from conventional magnets, as evidenced by their exotic excitations - such as pointlike monopoles or extended Dirac strings [4] - whose collective behavior we are only beginning to understand [4–9]. In particular, their dynamics is subject to the vagaries of the interplay of the unusual nature of the degrees of freedom with the subtle effects of other interaction terms that are inevitably

*Corresponding author: sag@iflysib.unlp.edu.ar
†Corresponding author: dtennant@utk.edu; present address: University of Tennessee Knoxville, Knoxville, Tennessee 37996, USA.

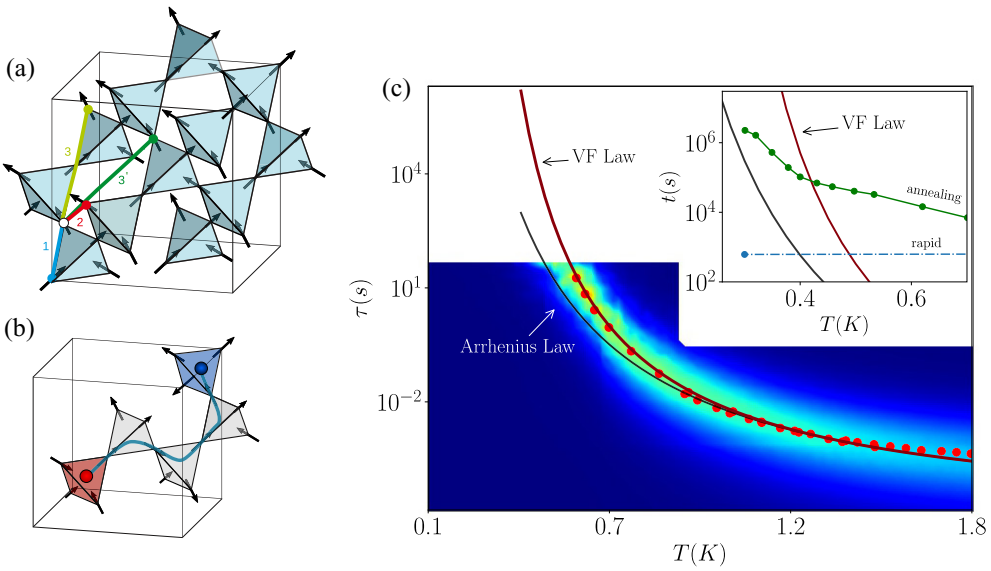

FIG. 1. Magnetic structure, monopole hopping, and relaxation time of DTO. (a) The spins in DTO are located on a pyrochlore lattice. The magnetic interaction pathways are shown in color, and dipolar coupling (not shown) is also important. These constrain the spin configurations to follow two-in/two-out ice rules. Breaking the ice rules results in the creation of a monopole antimonopole pair which can separate, creating a Dirac string as shown in (b). Monopoles are constrained by the other spins (Dirac strings) to travel over a restricted manifold. (c) Relaxation time (τ) for DTO extracted from noise measurements follows a Vogel-Fulcher-Tammann (VF) behavior below 1.5 K, rather than an Arrhenius law. The color map is of $\chi''(\omega)$ whose maximum gives a measure of τ. The inset shows the cooling protocol for one cycle of the neutron experiments: the symbols correspond to the waiting times as a function of temperature for the rapid (light blue) and slow cooling (green) protocols of the neutron experiments. These are compared with the VF law obtained from the noise and with the Arrhenius law fit to the data.

present in real materials and give rise to an intricate energy landscape.

$Dy_2Ti_2O_7$ (DTO) is a spin-ice material that belongs to the family of pyrochlore oxides of type $A_2^{3+}B_2^{4+}O_7^{2-}$ containing a wide range of highly frustrated magnets, many of which fail to order at low temperatures [4–7,10–12]. The magnetic lattice is shown in Fig. 1(a). Ising spins are located on the corners of tetrahedra and are restricted to pointing in- and outward. Recent experimental results demonstrated that a comprehensive fit to several thermodynamic properties [13–16] requires a Hamiltonian with exchange interactions to third nearest neighbors (as indicated in the figure), along with longer-ranged dipolar interactions. The resulting constrained states mentioned above are described by the ice rules, which stipulate two spins pointing in, and two out, at each tetrahedron [17,18]. Mapping spin vectors to an emergent magnetic field B gives a divergence-free condition, $\nabla \cdot B = 0$, reminiscent of magnetic fields in conventional magnetostatics. Indeed, if the ice rules are broken, say by a thermal single spin-flip excitation, then two topological defects (a pair of oppositely charged magnetic monopoles) form, and as they separate, they turn spins over along the way forming a Dirac string [see Fig. 1(b)]. Pure spin ice is in a Coulomb phase where the monopoles are deconfined, interacting through an emergent $1/r$ potential, as expected for charges in "free space," with the spin correlations having the functional form of free dipoles [4]. A central scientific question is how perturbing pure spin ice and reducing thermal disorder generates complex forms of matter such as glasses.

In this work we investigate the regime in which memory effects appear in $Dy_2Ti_2O_7$, at temperatures *much higher* than any predicted underlying ordering temperature [1]. We study this history dependence in a detailed neutron-scattering study incorporating different cooling protocols, connecting these results with extant magnetic susceptibility and noise measurements. Our numerical modeling indicates that this "supercooled"-liquid-like behavior is intimately connected to the passage of monopoles in an energy landscape that is *not quite* flat: interactions that at low enough temperatures induce order affect the potential landscape explored by monopoles as they hop from site to site, slowing down their dynamics at the same time as their density plummets. We model the resulting monopole pathways numerically, contrasting the regime where the spin network ultimately becomes glassy with the behavior of a robustly ordered magnet.

II. RESULTS

A. Spin interactions and glassiness

As DTO is cooled, the spin dynamics undergoes drastic slowing down, with the appearance below $T_{\rm irr} \approx 600$ mK of history dependence—typically evidenced by a divergence between field-cooled (FC) and zero-field-cooled (ZFC) magnetization measurements—and a host of accompanying phenomena such as thermal runaway [19–29]. The temperature dependence of a characteristic relaxation time, $\tau(T)$, can thus be extracted, with Fig. 1(c) showing the values from the most recent magnetic noise experiments [1], which are in good agreement with previously determined values (e.g., from [20,30,31]). Fitting a functional form is complicated by the temperature dependence of various physical processes involved in the dynamics. An Arrhenius law (black curve)

departs significantly from the data below approximately 800 mK. Instead, $\tau(T)$ can be well-fitted by a Vogel-Fulcher-Tammann (VF) form, $\tau(T) = \tau_0 \exp(A/(T - T_{\rm VF}))$, common for glasses (see, e.g., [32,33]), with $\tau_0 = 7.0(3) \times 10^{-6}s$, $T_{\rm VF} = 0.18(2)K$, and $A = 6.0(9)K$ (red curve), across all of the accessible temperature range (for a similar analysis of Monte Carlo simulation data see the Supplemental Material, SM [34]). The VF law *a priori* reflects cooperative effects rather than single-ion physics. $T_{\rm VF}$ is the Vogel divergence temperature, where the system reaches an infinite relaxation time. The figure also shows a color map of χ'' obtained from noise measurements [1] by means of the fluctuation dissipation theorem, whose maximum also gives a measure of τ. Measurements at temperatures and on timescales below and to the left of $\tau(T)$, respectively, probe the out-of-equilibrium behavior. At around 600 mK, the relaxation time is close to 200 s, and it rises swiftly below that temperature, exceeding 10^5 s below 300 mK.

A previous machine-learning study by a subset of the present authors identified an effective spin-ice Hamiltonian that, in the manner of Refs. [13–15], consists of a dipolar interaction combined with exchange terms up to third nearest neighbors (which are of two different kinds in the pyrochlore lattice). A prolate spheroid in parameter space was determined inside which several experimental observations, such as neutron scattering, specific heat, and magnetization, were well described by the model. Notably, this model, when simulated using a single spin-flip algorithm (SSF), successfully captures dynamical features of the system, such as the FC-ZFC irreversibility at 600 mK [21,35]. And if the standard correspondence between Monte Carlo (MC) steps and real time is used, it can also reproduce the departure from Arrhenius behavior in the magnetic relaxation timescale, as shown in the SM [36].

To probe the nature of this freezing we measure diffuse neutron-scattering spectra under different cooling protocols, "annealing" with a timescale of several days, as well as rapid cooling over an hour. The full temperature histories of two independent cooling cycles used for these measurements are shown in Fig. S1 of the SM [37]. Both cycles give identical results, so we focus our discussion on the longer one (cycle 2), with an annealing time close to a month (data for cycle 1 is shown in the SM [38]). The inset of Fig. 1(c) shows in logarithmic scale the waiting times at each temperature for each cooling protocol in this cycle, compared with the characteristic times from the VF and Arrhenius laws, as the temperature is lowered towards 300 mK. According to the VF law, even the longest waiting time, which slightly exceeds those of previous long-cooldown experiments ([31,39]), is out of equilibrium below 450 mK. The data from the neutron-scattering experiments supports this statement. As seen in Fig. 2(a), rapid and annealed cooldowns give indistinguishable scattering patterns (see SM [38] for a comparison and subtraction of raw data for cycle 1). This is also in agreement with the results seen in Ref. [39].

We find that the effective Hamiltonian gives an accurate quantitative description of the experimental neutron-scattering data, both after rapid cooling and annealing [Fig. 2(b)]. In accordance with the experiments, simulations of the diffuse scattering show Coulombic correlations associated with the emergent $U(1)$ gauge field between 2 and 1 K [Fig. 2(c)]. At lower temperatures, a further build-up in correlations is reflected in a sharpening of the features. Below 600 mK the correlations remain largely unchanged as one would expect for a glass, with no appreciable features indicating the development of long-range order, as opposed to numerical simulations using nonlocal updates where Bragg peaks develop at very low temperatures [13–15,19,35]. A calculated spin configuration below $T_{\rm irr}$ is shown in Fig. 3(a), whose structure factor matches the experimental NS data accurately [Fig. 2(b)]. To visualize the spatial magnetic correlations in the system, we use colored smooth surface wrappings around regions of connected tetrahedra with the same net magnetic moment. Ice rules allow six possible such orientations. For clarity, only four types are shown.

While computationally intensive, effective Hamiltonians open the possibility of investigating possible mechanisms by which the cooperative contribution to spin freezing might occur.

B. Monopole motion and domain formation

The simulations show spin dynamics in three distinct regions (illustrated in Fig. 4). In the liquid, $T > T_{\rm irr}$, monopole pathways overlap and are three dimensional. Short-range ferromagnetic clusters undergo bursts of rapid change as they are traversed by monopoles; over time the entire simulated volume reaches equilibrium (see Movie S1). In the intermediate region ($T_{\rm VF} < T < T_{\rm irr}$) the monopoles travel on sparse networks. The monopoles are then confined in intertwined FM regions, with the simulation timescale shorter than that on which large-scale spin rearrangements happen. Here monopole motion causes only local fluctuations of the clusters but not volume equilibration (Movie S2). At the lowest temperatures ($T < T_{\rm VF}$), the pathways are short and spatially confined, i.e., effectively zero dimensional. The monopoles have been reduced to short-range hops and the structure has hardened (Movies S3 and S4).

Supporting quantitative analysis, including monopole lifetimes, displacement, fractional visitation of sites, jumping rates, as well as quantification of looping of the pathways (using the first Betti number $N_{\rm Betti}$ [40]), is provided in the SM [41].

Our choice to represent magnetic correlations in terms of FM regions preserves the full microscopic information of the ice states but does not reflect the low-temperature ordered state of the model, which is of the Melko-Gingras type (see Refs. [14,15,19]). We note, however, that monopole motion is constrained to follow Dirac strings, i.e., it occurs preferentially along/opposite to (depending on the sign of the charge) the direction of the ferromagnetic moments, so that the time dependence of the FM domains provides a natural window into the dynamical processes in these systems.

Interactions modify the short-range structures and therefore the character and effective geometry of the pathways. Notably, the third-nearest-neighbor interaction plays a significant role in determining the low-temperature phase of this material. Figure 3(b) shows the simulated heat capacity over temperature C_v/T as a function of temperature along a straight line in the $J_3 - J_{3'}$ plane defined by ($J_{3'} - J_3 = 0.047$ K),

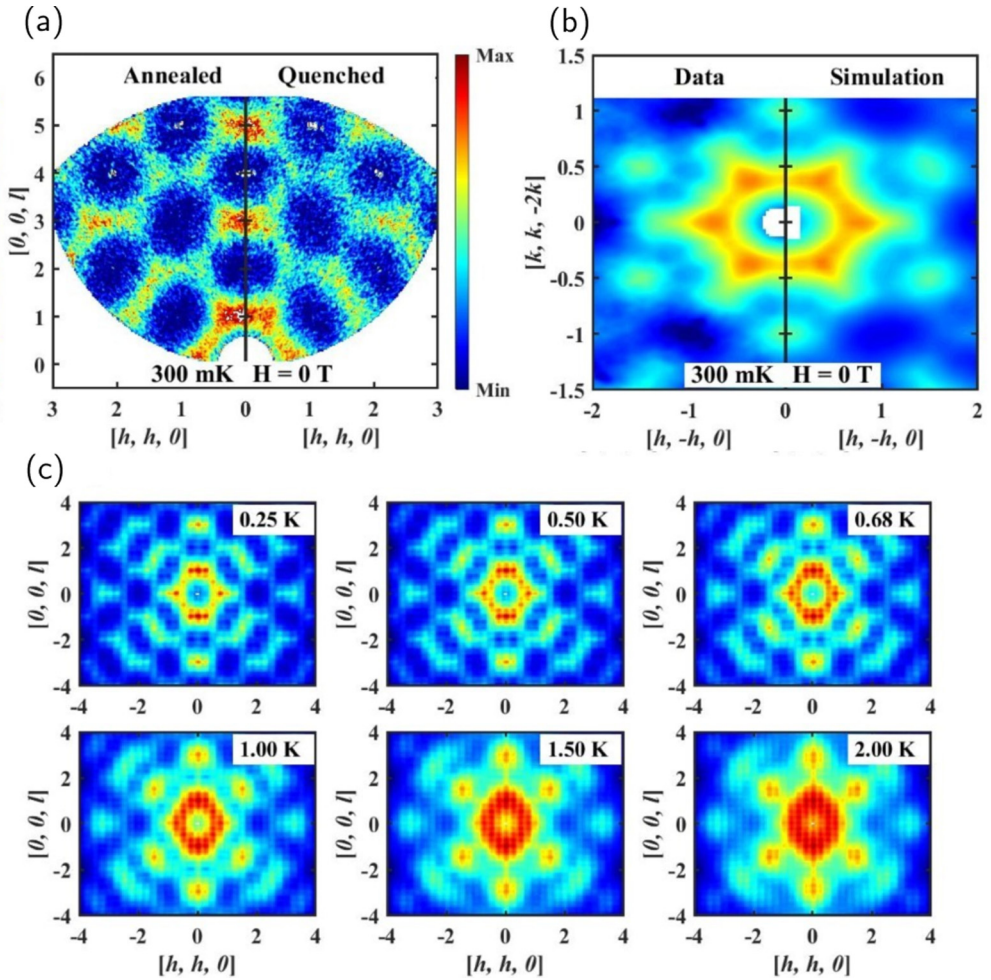

FIG. 2. Glass behavior in DTO. (a) Fast (1 hour) and slow ("annealed" over 4 weeks) cooling data, taken along trajectories indicated in Fig. 1(c) (inset), show little discernible difference (the measurements correspond to points A2 and R2 in the sample temperature history given in the SM [37]). (b) Modeled and measured (rapid cooled) diffuse scattering agree at low temperature. (For details on the neutron-scattering measurements and quantitative line-cut comparisons, see SM [42].) (c) Simulations of the diffuse scattering show Coulombic correlations associated with the Coulomb spin liquid at 1–2 K. At lower temperatures the buildup in correlations is reflected in a sharpening of the correlations. Below 600 mK the correlations remain largely unchanged, as expected for a glass. The simulations correspond to a Hamiltonian with dipolar interactions and up to third-nearest-neighbor exchange interactions with $D = 1.3224$ K, $J_1 = 3.41$ K, $J_2 = 0$, $J_3 = -0.004$ K, and $J_3' = 0.044$ K (for details see SM [43]).

with $J_3\prime$ ranging from -0.15 K to 0.22 K. The order that exists at both ends of the diagram, marked by a peak in C_v/T that decreases in temperature towards the center, is interrupted in a broad region between -0.1 and 0.3 K, where the system enters a glassy state at a roughly constant temperature. Our model for DTO lies at the center of this broad glassy region; this is a robust, rather than fine-tuned situation, that gives some latitude in the choice of parameters. The ferromagnetic clustering and, consequently, the character of the monopole pathways are also strongly dependent on J_3 and $J_3\prime$. Figure 3(c) shows the distribution of one region (colored yellow), alongside the monopole pathways, for different strengths of the third-neighbor couplings, marked as dotted lines in the phase diagram of Fig. 3(b). For negative J_3 and $J_3\prime$, panel [1] in Fig. 3(c), the low-temperature phase is ordered and the domains form parallel planes along two principal axes; as $J_3\prime$ increases towards the value for DTO (panel [DTO]), the system exhibits a broader disordered low-temperature phase, reflected in the regions becoming rugged and distributed across the whole sample. When $J_3\prime$ is further increased, the regions become progressively ordered, panel [2] in 3(c), and eventually, when the system orders at low temperature, they form a uniform crisscross pattern, panel [3] in 3(c). The right column shows the pathways for two monopoles in each case.

The frustrated DTO thus sits, as expected, in a region with a complex balance between dipolar, near, and further neighbor interactions; here, small changes in temperature significantly alter the morphology of the monopole pathways. This results in different dynamical behavior, which is seen in the simulations in a non-Lorentzian noise spectral density with a temperature-dependent anomalous exponent. The simulated noise spectrum, with a single spin-flip rate, matches qualitatively but not quantitatively with that of the experiments. As discussed in a recent work [1], a detailed modeling of the dynamics requires consideration of both cooperative behavior and the local physics of the spin-flipping process. While this

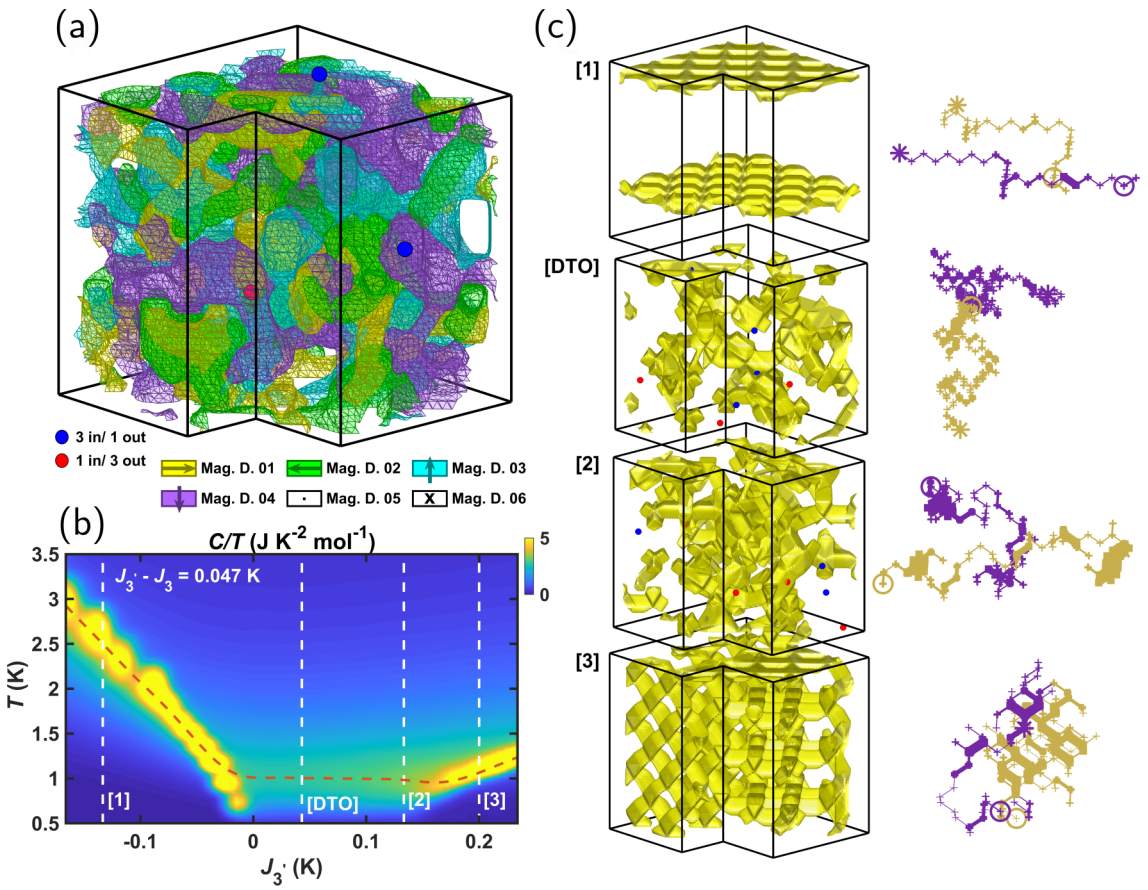

FIG. 3. Spin configurations and monopole trajectories as a function of third-neighbor interaction strength. (a) Connected tetrahedra with the same net magnetic moment define ferromagnetic (FM) regions, depicted by the smooth surface wrapping around them. Ice rules allow six FM orientations. The configuration here is modeled at $T = 300$ mK $< T_{\rm irr}$ using parameters from Ref. [16], see text. For clarity, only four FM orientations are shown. Monopoles are trapped in this structure, as can be seen in the animation of the time dependence presented in SI (Movie S1). (B) Calculated heat capacity over temperature (C_v/T) along the line $J_3 - J_{3\prime} = 0.047$ K, plotted as a function of $J_{3\prime}$ and T. Order is seen at either limit, interrupted by glass formation in a broad intermediate region. The glass formation occurs at a near-constant temperature which disrupts order at its characteristic temperature. (c) The morphology of the FM regions changes with third-nearest-neighbor interactions. A single type of FM region is shown for the parameters indicated by vertical dashed lines in (b). This shows the influence of different ordering tendencies. To the right of each subfigure, a pair of corresponding typical monopole pathways is shown.

is necessary to accurately describe the noise spectrum, they do not alter the morphology of monopole pathways.

C. Physical origin of glass formation

Our results suggest an interpretation where glass forms from a combination of rarefaction of monopoles and the build-up of short-range correlations in turn restricting their motion. These correlations appear to be brought about by precursors to ordering that would eventually occur in thermodynamic equilibrium at lower temperatures – thus producing a remarkable instance of frustrated phase ordering kinetics preceding the ordering temperature.

With cooling, large-scale annealing events, where many monopoles exchange position in bursts and the effective potential landscape changes akin to an avalanche, are unlikely to be sampled in any experimental timescale. Measurements instead reflect the common short-ranged excursions of monopoles which result in fluctuations around, rather than changes of, a given ice configuration. As temperature decreases, even these motions are increasingly blocked and below $T_{\rm VF}$ annealing is effectively prevented as energy barriers are too large for monopoles to move between energy minima on experimentally accessible time scales.

Spin glasses are usually found in materials with randomness as well as frustration. Relaxor ferroelectrics are created as a result of strong ionic site disorder [44]. DTO on the other hand has no evident intrinsic randomness or disorder. Instead, it has much closer connection to structural glass behavior where networks of bonds, defects, and coordination are important. Some liquids, particularly those with high degrees of frustration, remain liquid down to low temperatures without crystallization, and become glassy due to kinetic slowdown [45]. In DTO similar behavior appears to occur because the primary couplings are large compared to the glass formation temperature, and the strong frustration stabilizes the liquid state down to low temperatures. The small perturbation of distant neighbor couplings then freeze the fragile domain

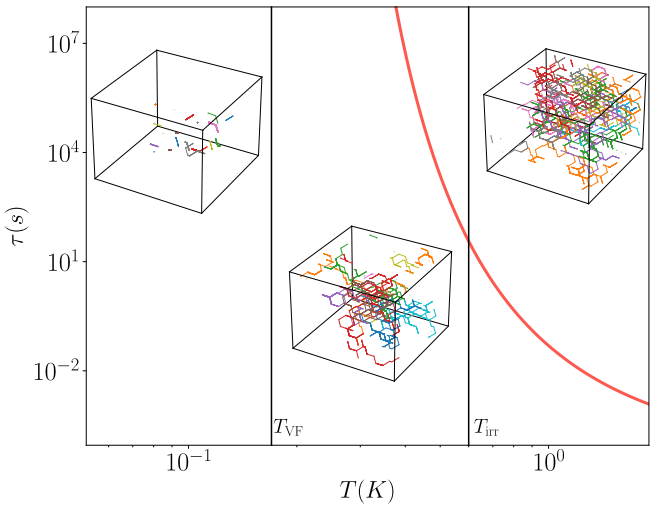

FIG. 4. Monopole pathways at different temperatures. For clarity of comparison, the same (artificially) fixed density of monopoles is shown at each temperature; in reality, the number of monopoles at lowest temperature is vanishingly small. The graph shows characteristic monopole paths taken over a finite MC time in three regions. Above the irreversibility line, $T > T_{irr}$, the monopole paths are extended and mutually connected and (eventually) span the whole sample. For $T_{VF} < T < T_{irr}$, the monopole pathways take the form of sparse networks; as temperature is lowered their size and dimensionality is increasingly reduced and they become disconnected. For $T < T_{VF}$ the monopoles are essentially frozen and the pathways become zero dimensional. The red line is the VF law that best fits the relaxation time data (shown in Fig. 1).

structure. The behavior of DTO below 800 mK resembles the development of dynamic heterogeneity in supercooled liquids [46,47]. Previous measurement of a VF law in spin ice was associated with a supercooled spin liquid [48]. The phase diagram in Fig. 3(b) does not indicate an avoided long-range ordering around 600 mK, and the equilibrium ordering temperature into a Melko-Gingras type crystal, found using loop algorithms in our model Hamiltonian, lies close to 200 mK. This temperature, unlike the case of supercooled liquids, coincides within experimental error with T_{VF}. This is a consequence of the freezing in the mobility of defects that occurs at crystallisation, which implies a divergence of the characteristic time.

III. DISCUSSION AND CONCLUSIONS

The nature of the low-temperature state of spin-ice materials has been a matter of continued investigation. As T is lowered into the spin-ice phase, characteristic Coulomb correlations appear that can be described by a dipolar spin-ice model. Crucially, however, the behavior of the "pure" version of this ice model, and its varieties, differ greatly in this regime. What is special about the dipolar spin-ice model is that its constrained manifold of the exponentially many degenerate states obeying the ice rules is very "flat"; in a slightly simplified model, such as the dumbbell model [4], all these states are degenerate. The motion of the monopoles, which connects these states, thus takes place without encountering significant energy barriers and only slows down as the size of the monopole population is thermally suppressed, following an Arrhenius law [49]. Corrections to the point charge approximation of the monopoles and further neighbor exchange interactions, however, select a subset of ground states which is generically small and involves spontaneous (at least partial) ordering at even lower temperatures. It is a much investigated and long-standing issue in the physics of spin ice that such ordering has never been observed experimentally. Our observations advocate the view that these subdominant interactions generate obstacles to the monopole motion by endowing the previously flat energy landscape with additional structure; this is the frustrated kinetics in the constrained manifold arising from the ice rules. It is in this sense that we refer to spin ice as a structural magnetic glass. Like a structural glass, its slow, non-Arrhenius dynamics can be the result not of disorder or boundary effects [50] but of a nontrivial energy landscape arising as a cooperative effect.

The high tunability of magnetic materials like DTO with pressure and chemical substitution, their simple and well-defined interactions, and lattice nature make them highly attractive as a route to understanding the complex physics behind structural glasses. In these materials, the remarkable physics of partially disordered phases of matter and how they emerge from competition is well suited to machine learning. This can be applied to spin simulations directly and may provide surprising new insights. Highly degenerate manifolds are increasingly being studied in topological and quantum materials, and the findings here should be highly relevant. Spin jammed states [51–55] have been proposed in frustrated magnets, and disordered states appear to compete with potential quantum spin liquids. In addition, narrow-band electronic systems are being explored that will also have large degenerate manifolds if tuned to the Fermi energy [56]. These considerations are not limited to real materials but also extend to artificial magnetic arrays [57], where similar instances of slow dynamics and glassiness have been encountered in recent years [58].

In conclusion, the dipolar and small further neighbor interactions in spin ice $Dy_2Ti_2O_7$ appear to be responsible for the appearance of glassy dynamics. On cooling, short-range correlations emerge which introduce restrictions on monopole pathways. This eventually breaks the ergodicity of the system on measurement timescales at a temperature matching the irreversibility temperature, $T_{irr} \approx 600$ mK, and a glassy state exhibiting only the short-range correlations is formed. The dynamics gradually becomes yet more sluggish as the temperature drops further, and our fit of the relaxation time to a Vogel-Fulcher law leads to a temperature scale $T_{VF} \approx 200$ mK for its divergence, which is close to the numerically obtained thermodynamic transition temperature into a fully ordered state. The ordering tendencies and geometry of the pathways are shown to be controllable by the strength of further neighbor interactions. The simplicity of the model suggests that spin ice presents new opportunities for microscopic understanding of glass formation and a new platform to study glassy behavior.

The data and material that support the findings of this study are available from the corresponding author upon reasonable request.

ACKNOWLEDGMENTS

D.A.T. and A.M.S. would like to thank Cristian Batista and Erica Carlson for useful discussions. Funding: Z.L.D. and H.D.Z. thank the NSF for support with Grant No. DMR-2003117. A portion of this research used resources at Spallation Neutron Source and was supported by DOE BES User Facilities. This material is based upon work supported by the U.S. Department of Energy, Office of Science, National Quantum Information Science Research Centers, Quantum Science Center. Support for Q.Z. was provided by US DOE under EPSCoR Grant No. DESC0012432 with additional support from the Louisiana Board of Regents. The computer modeling used resources of the Oak Ridge Leadership Computing Facility, which is supported by the Office of Science of the U.S. Department of Energy under Contract No. DE-AC05-00OR22725. S.A.G. thanks Agencia Nacional de Promoción Científica y Tecnológica through PICT 2017-2347. This work was partly supported by the Deutsche Forschungsgemeinschaft under Grant No. SFB 1143 (Project ID No. 247310070) and the cluster of excellence ct.qmat (EXC 2147, Project ID No. 390858490), by the Helmholtz Virtual Institute, "New States of Matter and their Excitations," and by the Engineering and Physical Sciences Research Council (EPSRC) through Grants No. EP/K028960/1, No. EP/P034616/1, and No. EP/T028580/1 (C.C.). Part of this work was carried out within the framework of a Max-Planck independent research group on strongly correlated systems. T.E. was supported by the U.S. Department of Energy under Contract No. B97354X20, Office of Science, Basic Energy Sciences, Materials Sciences, and Engineering Division.

Author contributions. Conception of measurement D.A.T., S.A.G., and wider project D.A.T., S.A.G., C.C., R.M. Neutron scattering measurements S.A.G., A.S., D.A.T., B.K., R.F., M.M., Q.Z., Z.D., and H.Z. Modeling, analysis, and interpretation A.S., S.A.G., D.A.T., T.E., R.A.B., J.H., L.J., C.C., and R.M. Paper writing R.M., C.C., S.A.G., and D.A.T., with input from all coauthors.

The authors declare no competing interests.

[1] A. M. Samarakoon, S. A. Grigera, D. A. Tennant, A. Kirste, B. Klemke, P. Strehlow, M. Meissner, J. N. Hallén, L. Jaubert, C. Castelnovo, and R. Moessner, Anomalous magnetic noise in an imperfectly flat landscape in the topological magnet Dy2Ti2O7, Proc. Natl. Acad. Sci. **119**, e2117453119 (2022).

[2] L. Balents, Spin liquids in frustrated magnets, Nature (London) **464**, 199 (2010).

[3] J. Knolle and R. Moessner, A field guide to spin liquids, Annu. Rev. Condens. Matter Phys. **10**, 451 (2019).

[4] C. Castelnovo, R. Moessner, and S. L. Sondhi, Magnetic monopoles in spin ice, Nature (London) **451**, 42 (2008).

[5] D. J. P. Morris, D. A. Tennant, S. A. Grigera, B. Klemke, C. Castelnovo, R. Moessner, C. Czternasty, M. Meissner, K. C. Rule, J.-U. Hoffmann, K. Kiefer, S. Gerischer, D. Slobinsky, and R. S. Perry, Dirac strings and magnetic monopoles in the spin ice Dy2Ti2O7, Science **326**, 411 (2009).

[6] T. Fennell, P. P. Deen, A. R. Wildes, K. Schmalzl, D. Prabhakaran, A. T. Boothroyd, R. J. Aldus, D. F. McMorrow, and S. T. Bramwell, Magnetic Coulomb phase in the spin ice Ho2Ti2O7, Science **326**, 415 (2009).

[7] C. Castelnovo, R. Moessner, and S. Sondhi, Spin ice, fractionalization, and topological order, Annu. Rev. Condens. Matter Phys. **3**, 35 (2012).

[8] K. A. Ross, L. Savary, B. D. Gaulin, and L. Balents, Quantum Excitations in Quantum Spin Ice, Phys. Rev. X **1**, 021002 (2011).

[9] M. J. Gingras and P. A. McClarty, Quantum spin ice: A search for gapless quantum spin liquids in pyrochlore magnets, Rep. Prog. Phys. **77**, 056501 (2014).

[10] C. L. Henley, The Coulomb phase in frustrated systems, Annu. Rev. Condens. Matter Phys. **1**, 179 (2010).

[11] J. S. Gardner, M. J. P. Gingras, and J. E. Greedan, Magnetic pyrochlore oxides, Rev. Mod. Phys. **82**, 53 (2010).

[12] J. Rehn and R. Moessner, Maxwell electromagnetism as an emergent phenomenon in condensed matter, Philos. Trans. R. Soc. A **374**, 20160093 (2016).

[13] T. Yavors'kii, T. Fennell, M. J. P. Gingras, and S. T. Bramwell, Dy2Ti2O7 Spin Ice: A Test Case for Emergent Clusters in a Frustrated Magnet, Phys. Rev. Lett. **101**, 037204 (2008).

[14] R. A. Borzi, F. G. Albarracín, H. D. Rosales, G. L. Rossini, A. Steppke, D. Prabhakaran, A. Mackenzie, D. C. Cabra, and S. A. Grigera, Intermediate magnetization state and competing orders in Dy2Ti2O7 and Ho2Ti2O7, Nat. Commun. **7**, 12592 (2016).

[15] P. Henelius, T. Lin, M. Enjalran, Z. Hao, J. G. Rau, J. Altosaar, F. Flicker, T. Yavors' kii, and M. J. P. Gingras, Refrustration and competing orders in the prototypical Dy2Ti2O7 spin ice material, Phys. Rev. B **93**, 024402 (2016).

[16] A. M. Samarakoon, K. Barros, Y. W. Li, M. Eisenbach, Q. Zhang, F. Ye, V. Sharma, Z. L. Dun, H. Zhou, S. A. Grigera, C. D. Batista, and D. A. Tennant, Machine-learning-assisted insight into spin ice $Dy_2Ti_2O_7$, Nat. Commun. **11**, 892 (2020).

[17] M. J. Harris, S. T. Bramwell, D. F. McMorrow, T. Zeiske, and K. W. Godfrey, Geometrical Frustration in the Ferromagnetic Pyrochlore Ho2Ti2O7, Phys. Rev. Lett. **79**, 2554 (1997).

[18] S. T. Bramwell and M. J. P. Gingras, Spin ice state in frustrated magnetic pyrochlore materials, Science **294**, 1495 (2001).

[19] R. G. Melko, B. C. den Hertog, and M. J. P. Gingras, Long-Range Order at Low Temperatures in Dipolar Spin Ice, Phys. Rev. Lett. **87**, 067203 (2001).

[20] J. Snyder, J. Slusky, R. Cava, and P. Schiffer, How spin ice freezes, Nature (London) **413**, 48 (2001).

[21] J. Snyder, B. G. Ueland, J. S. Slusky, H. Karunadasa, R. J. Cava, and P. Schiffer, Low-temperature spin freezing in the Dy2Ti2O7 spin ice, Phys. Rev. B **69**, 064414 (2004).

[22] L. D. Jaubert and P. C. Holdsworth, Signature of magnetic monopole and Dirac string dynamics in spin ice, Nat. Phys. **5**, 258 (2009).

[23] D. Slobinsky, C. Castelnovo, R. A. Borzi, A. S. Gibbs, A. P. Mackenzie, R. Moessner, and S. A. Grigera, Unconventional Magnetization Processes and Thermal Runaway in Spin-Ice Dy2Ti2O7, Phys. Rev. Lett. **105**, 267205 (2010).

[24] L. D. C. Jaubert and P. C. W. Holdsworth, Magnetic monopole dynamics in spin ice, J. Phys.: Condens. Matter **23**, 164222 (2011).

[25] K. Matsuhira, M. Wakeshima, Y. Hinatsu, C. Sekine, C. Paulsen, T. Sakakibara, and S. Takagi, Slow dynamics of Dy pyrochlore oxides Dy2Sn2O7 and Dy2Ir2O7, J. Phys.: Conf. Ser. **320**, 012050 (2011).

[26] L. R. Yaraskavitch, H. M. Revell, S. Meng, K. A. Ross, H. M. L. Noad, H. A. Dabkowska, B. D. Gaulin, and J. B. Kycia, Spin dynamics in the frozen state of the dipolar spin ice material Dy2Ti2O7, Phys. Rev. B **85**, 020410(R) (2012).

[27] C. Paulsen, M. J. Jackson, E. Lhotel, B. Canals, D. Prabhakaran, K. Matsuhira, S. Giblin, and S. Bramwell, Far-from-equilibrium monopole dynamics in spin ice, Nat. Phys. **10**, 135 (2014).

[28] M. J. Jackson, E. Lhotel, S. R. Giblin, S. T. Bramwell, D. Prabhakaran, K. Matsuhira, Z. Hiroi, Q. Yu, and C. Paulsen, Dynamic behavior of magnetic avalanches in the spin-ice compound Dy2Ti2O7, Phys. Rev. B **90**, 064427 (2014).

[29] P. C. Guruciaga, L. Pili, S. Boyeras, D. Slobinsky, S. A. Grigera, and R. A. Borzi, Anomalous out-of-equilibrium dynamics in the spin-ice material $Dy_2Ti_2O_7$ under moderate magnetic fields, J. Phys.: Condens. Matter **32**, 425804 (2020).

[30] K. Matsuhira, C. Paulsen, E. Lhotel, C. Sekine, Z. Hiroi, and S. Takagi, Spin dynamics at very low temperature in spin ice Dy2Ti2O7, J. Phys. Soc. Jpn. **80**, 123711 (2011).

[31] D. Pomaranski, L. Yaraskavitch, S. Meng, K. Ross, H. Noad, H. Dabkowska, B. Gaulin, and J. Kycia, Absence of Pauling's residual entropy in thermally equilibrated Dy2Ti2O7, Nat. Phys. **9**, 353 (2013).

[32] S. Shtrikman and E. Wohlfarth, The theory of the Vogel-Fulcher law of spin glasses, Phys. Lett. A **85**, 467 (1981).

[33] L. S. Garca-Coln, L. F. del Castillo, and P. Goldstein, Theoretical basis for the Vogel-Fulcher-Tammann equation, Phys. Rev. B **40**, 7040 (1989).

[34] See Supplemental Material at http://link.aps.org/supplemental/10.1103/PhysRevResearch.4.033159 for a similar analysis of Monte Carlo simulation data.

[35] L. Bovo, M. Twengström, O. Petrenko, T. Fennell, M. Gingras, S. Bramwell, and P. Henelius, Special temperatures in frustrated ferromagnets, Nat. Commun. **9**, 1999 (2018).

[36] See Sec. III of Supplemental Material at http://link.aps.org/supplemental/10.1103/PhysRevResearch.4.033159 for Vogel-Fulcher behavior in Monte Carlo simulations.

[37] See Fig S1 in Supplemental Material at http://link.aps.org/supplemental/10.1103/PhysRevResearch.4.033159.

[38] See Fig S2 of Supplemental Material at http://link.aps.org/supplemental/10.1103/PhysRevResearch.4.033159 for rapid and slow cooldown data for cycle 1.

[39] S. R. Giblin, M. Twengstrom, L. Bovo, M. Ruminy, M. Bartkowiak, P. Manuel, J. C. Andresen, D. Prabhakaran, G. Balakrishnan, E. Pomjakushina, C. Paulsen, E. Lhotel, L. Keller, M. Frontzek, S. C. Capelli, O. Zaharko, P. A. McClarty, S. T. Bramwell, P. Henelius, and T. Fennell, Pauling Entropy, Metastability, and Equilibrium in Dy2Ti2O7 Spin Ice, Phys. Rev. Lett. **121**, 067202 (2018).

[40] A. Hatcher, *Algebraic Topology* (Cambridge University Press, Cambridge, England, 2002).

[41] See Sec. II D of Supplemental Material at http://link.aps.org/supplemental/10.1103/PhysRevResearch.4.033159 for a quantitative analysis of monopole pathways.

[42] See Supplemental Material at http://link.aps.org/supplemental/10.1103/PhysRevResearch.4.033159 for details on the neutron-scattering measurements and quantitative line-cut comparisons.

[43] See Sec. II of Supplemental Material at http://link.aps.org/supplemental/10.1103/PhysRevResearch.4.033159 for details on the parameter determination.

[44] L. E. Cross, Relaxor ferroelectrics, Ferroelectrics **76**, 241 (1987).

[45] P. G. Debenedetti and F. H. Stillinger, Supercooled liquids and the glass transition, Nature (London) **410**, 259 (2001).

[46] M. D. Ediger, Spatially heterogeneous dynamics in supercooled liquids, Annu. Rev. Phys. Chem. **51**, 99 (2000).

[47] S. C. Glotzer, V. N. Novikov, and T. B. Schrøder, Time-dependent, four-point density correlation function description of dynamical heterogeneity and decoupling in supercooled liquids, J. Chem. Phys. **112**, 509 (2000).

[48] E. R. Kassner, A. B. Eyvazov, B. Pichler, T. J. Munsie, H. A. Dabkowska, G. M. Luke, and J. S. Davis, Supercooled spin liquid state in the frustrated pyrochlore Dy2Ti2O7, Proc. Natl. Acad. Sci. **112**, 8549 (2015).

[49] V. Lubchenko and P. G. Wolynes, Theory of structural glasses and supercooled liquids, Annu. Rev. Phys. Chem. **58**, 235 (2007).

[50] H. Revell, L. Yaraskavitch, J. Mason, K. Ross, H. Noad, H. Dabkowska, B. Gaulin, P. Henelius, and J. Kycia, Evidence of impurity and boundary effects on magnetic monopole dynamics in spin ice, Nat. Phys. **9**, 34 (2013).

[51] P. Chandra, P. Coleman, and I. Ritchey, The anisotropic kagome antiferromagnet: A topological spin glass?, J. Phys. I **3**, 591 (1993).

[52] A. Samarakoon, T. J. Sato, T. Chen, G.-W. Chern, J. Yang, I. Klich, R. Sinclair, H. Zhou, and S.-H. Lee, Aging, memory, and nonhierarchical energy landscape of spin jam, Proc. Natl. Acad. Sci. **113**, 11806 (2016).

[53] T. Bilitewski, M. E. Zhitomirsky, and R. Moessner, Jammed Spin Liquid in the Bond-Disordered Kagome Antiferromagnet, Phys. Rev. Lett. **119**, 247201 (2017).

[54] T. Bilitewski and R. Moessner, Disordered flat bands on the kagome lattice, Phys. Rev. B **98**, 235109 (2018).

[55] J. G. Rau and M. J. Gingras, Spin slush in an extended spin ice model, Nat. Commun. **7**, 12234 (2016).

[56] M. Kang, L. Ye, S. Fang, J.-S. You, A. Levitan, M. Han, J. I. Facio, C. Jozwiak, A. Bostwick, E. Rotenberg *et al.*, Dirac fermions and flat bands in the ideal kagome metal FeSn, Nat. Mater. **19**, 163 (2020).

[57] P. Schiffer and C. Nisoli, Artificial spin ice: Paths forward, Appl. Phys. Lett. **118**, 110501 (2021).

[58] S. H. Skjærvø, C. H. Marrows, R. L. Stamps, and L. J. Heyderman, Advances in artificial spin ice, Nat. Rev. Phys. **2**, 13 (2020).